



Article

# The Effect of Lateral Load Type on Shear Lag of Concrete Tubular Structures with Different Plan Geometries

Mostafa Moghadasi <sup>1,\*</sup>, Soheil Taeepoor <sup>2</sup>, Seyed Saeid Rahimian Koloor <sup>3</sup> and Michal Petruš <sup>3</sup>

<sup>1</sup> Department of Civil Engineering, Faculty of Engineering, Bu-Ali Sina University, Hamedan 6516738695, Iran

<sup>2</sup> M.Sc. Graduated, Department of Civil Engineering, Faculty of Engineering, Islamic Azad University, South Tehran, Tehran 1584743311, Iran; soheiltaeepoor@ymail.com

<sup>3</sup> Institute for Nanomaterials, Advanced Technologies and Innovation (CXI), Technical University of Liberec (TUL), Studentska 2, 461 17 Liberec, Czech Republic; s.s.r.koloor@gmail.com (S.S.R.K.); michalpetrus@tul.cz (M.P.)

\* Correspondence: m.moghadasi@basu.ac.ir

Received: 3 September 2020; Accepted: 30 September 2020; Published: 3 October 2020



**Abstract:** Tubular structures are extensively recognized as a high efficiency and economically reasonable structural system for the design and construction of skyscrapers. The periphery of the building plan in a tubular system consists of closely spaced columns connected by circumferential deep spandrels. When a cantilever tube is subjected to a lateral load, it is expected that the axial stress in each column located in the flange frame of the tube is the same, but because of the flexibility of peripheral beams, the axial stress in the corner columns and middle columns is distributed unequally. This anomaly is called “shear lag”, and it is a leading cause of the reduction in efficiency of the structure. In this paper, the possible relation between shear lag and the type of lateral load subjected to these systems is investigated. The above relation is not yet considered in previous literatures. Three various plan shapes including rectangular, triangular and hexagon were modeled, analyzed, designed and subjected to the earthquake and wind load, separately. Further work is carried out to compare the shear lag factor of these structures with distinct plan shapes against different types of lateral load. It is observed that all types of structures with various plan geometry subjected to the wind load had a greater amount of shear lag factor in comparison with structures subjected to the static and dynamic earthquake loads. In addition, shear lag in structures with the hexagon shaped plan was at the minimum.

**Keywords:** tall building; framed tube; lateral load type; plan geometry; shear lag; structural behavior

## 1. Introduction

The framed tube idea is an effective framing system for high-rise buildings. This type of structural system is mainly comprises closely spaced circumferential columns, which are connected by deep spandrel beams. The whole system works as a giant vertical cantilever, and its high efficiency is due to the large distance between windward and leeward columns. Among the most important specifications of tubular systems is their high economic efficiency. A case in point is that the material consumed in this kind of system is reduced by half in comparison with other systems [1]. In a rigid frame the “strong” bending direction of columns is aligned perpendicular to the face, while this factor is typically aligned along the face of the building in a framed tube system. In a framed tube system, the tube form resists overturning produced by lateral load—a leading cause of compression and tension in columns. Bending in columns and beams or rotation of the beam-column joint in the web section resists the

shear force produced by lateral load. Gravity loads are resisted partly by exterior frames and partly by interior columns [2].

In an ideal tubular structure, circumferential columns and beams are assumed to be completely rigid, so both web and flange panels act separately and bend against lateral loads like a true cantilever. While the above system has a tubular form, it also has a more complicated behavior than a solid tube. To be more specific, the components in a framed tube cannot be completely rigid due to technical and economic constraints [3]. This will be a leading cause of nonuniform distribution of loads in columns.

Consequently, in a framed-tube structure under lateral load, the stress distribution in the flange wall panels is nonuniform and is nonlinear in the web wall panels. This anomaly which reduces the efficiency of the structures is referred to as “shear lag” [4]. To obtain a better understanding of this phenomenon, a factor called the shear lag factor is defined. This factor is a ratio of the corner column axial force to the middle column axial force. When the stresses in the corner columns of the flange frame panels exceed those in the middle columns, the shear lag is positive. Nevertheless, in some cases, it is vice-versa where the stress in the middle columns exceeds those in the corner columns, and this is referred to as the negative shear lag.

This paper studied the effect of lateral load type on the shear lag phenomenon in framed-tube reinforced concrete tall buildings with different plan geometries.

## 2. Review of Literature

With regard to the great importance of framed tube systems in the construction of high-rise buildings, it is no wonder that multifarious research has been carried out on this structural system and its shortcomings in order to make framed tube systems more effective. However, previous studies did not pay enough attention to the subjected load type and its relation to the shear lag factor and the shape of the structures, which play an important role in the amount of this factor.

In 1969, Fazlur Khan proposed a chart named “structural systems for height” which has classified the different types of tubular systems with regard to their efficiency for high-rise buildings of different heights [5]. In the same year, Chang and Zheng tried to find out more about negative shear lag and its influential factors on a cantilever box girder. In this research, they found that negative shear lag will change with the different boundary conditions of displacement and external force applied to the girder [6]. In 1988, Shiraishi et al. studied the aerodynamic stability effects on rectangular cylinders by altering their shapes subjected to the lateral loads such as wind and water flow. They cut some squares with different sizes in each edge in a rectangular cross section and observed that it has a controlling effect on the separated shear layer generating from the leading edge. These sections with various sizes of corner-cuts had totally different behaviors against wind force and water flume [7]. In 1990, Hayashida and Iwasa investigated the effects of the geometry of structures on aerodynamic forces and displacement response for tall buildings. They tested four different plan shapes, with and without corner-cuts in a wind tunnel and identified the aerodynamic damping effects produced by changing some parts of the basic cross section and also the aerodynamic character of basic shapes [8]. In 1991, Connor and Pouangare presented a simple model for the design of framed tube structures. They modeled the structures as a series of stringers which resisted axial forces without bending rigidity and shear panels which resisted shear forces without bending or axial rigidity. They proposed a model that gives accurate results for the preliminary design and analysis of tubular structures with different geometry and material properties [9]. Kwan, in 1994, proposed a hand calculation method for approximate analysis in framed tube structures by considering the shear lag factor. This method could be useful for preliminary design and quick evaluation and could provide a better perception of the effect of multifarious parameters on the structure’s behavior [10]. In 2000, Han et al. investigated the shear lag factor in the web panels of shear-core walls [11]. Lee et al., in 2002, looked into the behavior of the shear lag of framed tube structures with and without internal tube(s) for the behavioral characteristics of the structures and also the relation between their performance and various structural parameters. They also proposed a simple numerical method for the prediction of the shear lag effect in

framed tube structures. It has been found that the stiffness factor has an effective role in producing shear lag in tubular structures [12]. Haji-Kazemi and Company proposed a new method to analyze shear lag in framed tube structures using an analogy between the shear lag behavior of a cantilever box which represents a uniform framed tube building. This method is able to accurately analyze positive as well as negative shear lag effects in tubular structures accurately [13]. Furthermore, Moghadasi and Keramati, in 2009, studied the effects of internal tubes in shear lag reduction. They reduced the lateral displacement and shear lag amount in high-rise buildings by adding internal tubes to the framed tube structures [14].

In 2012, Shin et al. investigated different parameters such as depth and width of beams and columns on the behavior of shear lag in a frame-wall tube building. The results showed that the effect of column depth on the shear lag behavior of framed tube was more outstanding than other parameters [15]. In 2014, Mazinani et al. compared the shear lag amount of pure tube structural systems with braced tube systems and different types of X-diagonal bracing. It was observed that these braces started from corner-to-corner, increased the stiffness of the structure and consequently reduced the story drift and shear lag factor in the tubular system [16]. In addition, Nagvekar and Hampali studied the shear lag phenomenon in both the web and wing panel of a hollow structure and measured it in various heights of a structure [17]. The plan geometry, building's body form, the ratio of height to width and three-dimensional stiffness for the transfer of wind and seismic loads are the most important structural system properties affect the behavior of tall buildings, as reported by Szolomicki and Golasz-Szolomicka [18]. Alaghmandan et al. in 2016 inquired about the architectural strategies on wind effects in tall buildings. These tactics included altering the geometry of the whole building scale such as tapering and setbacks, and attenuated the wind effects in some models by architectural strategies [19]. In 2019, Shi and Zhang proposed a simplified method for calculation of shear lag in diagrid framed tube structures. In their study, the diagrid tube structure is assumed to be equivalent to continuous orthogonal elastic membrane. They tried to solve two key problems of finding the optimized angle of the diagonal column and the shear lag assessment in the preliminary design of the above structures [20].

In terms of microstructural view of concrete subjected to dynamic loading at high strain rates, Hentz et al. used a 3D discrete element method and verified it [21]. Furthermore, the evaluation of concrete cracks occurring in complex states of stress was studied by Golewski and Sadowski [22]. In their study, crack development at shear was investigated through experimental tests using two types of aggregates.

As seen from the review above of previous studies, the possible relation between shear lag and the type of lateral load subjected to these systems is not yet considered.

### **3. Structural Models and Analyses Specifications**

#### *3.1. Characteristics and Final Dimensions*

In this paper, 12 reinforced concrete framed tube buildings with different heights and different shapes are modeled and analyzed. From a shape point of view, they were divided into three various groups of structures with (a) rectangular, (b) triangular and (c) hexagonal plan shapes (See Figure 1). Each structural plan shape consists of four different heights: 20-story, 40-story, 60-story and 80-story buildings. Figure 2 shows example pictures of each type of buildings illustrated in Figure 1. Table 1 shows the terminology of the models used in this paper. Figure 3 displays the 40-story models in ETABS software version 18.1.1 as examples. This software is chosen because it is developed specifically for the analysis and design of building structures. Furthermore, it has a high ability for static and dynamic analyses regardless of the number of nodes and stories.

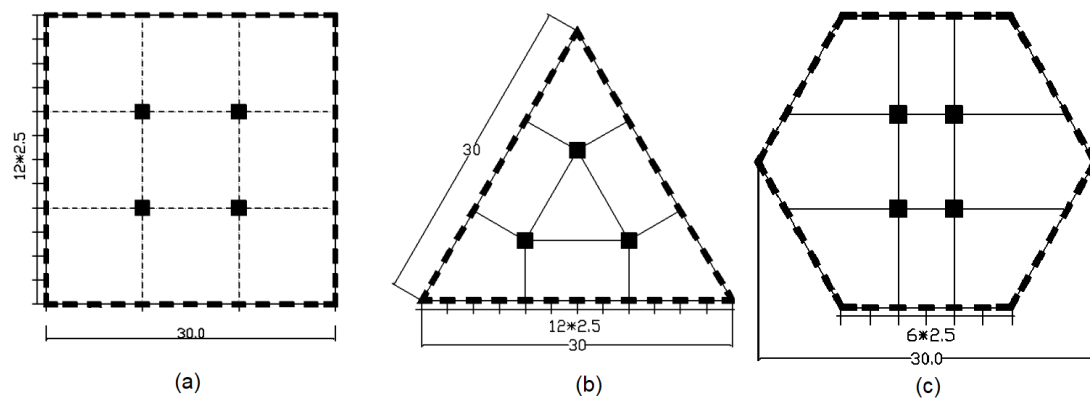


**Figure 1.** Three different plan shapes: (a) rectangular, (b) triangular and (c) hexagonal (all dimensions are in meters).

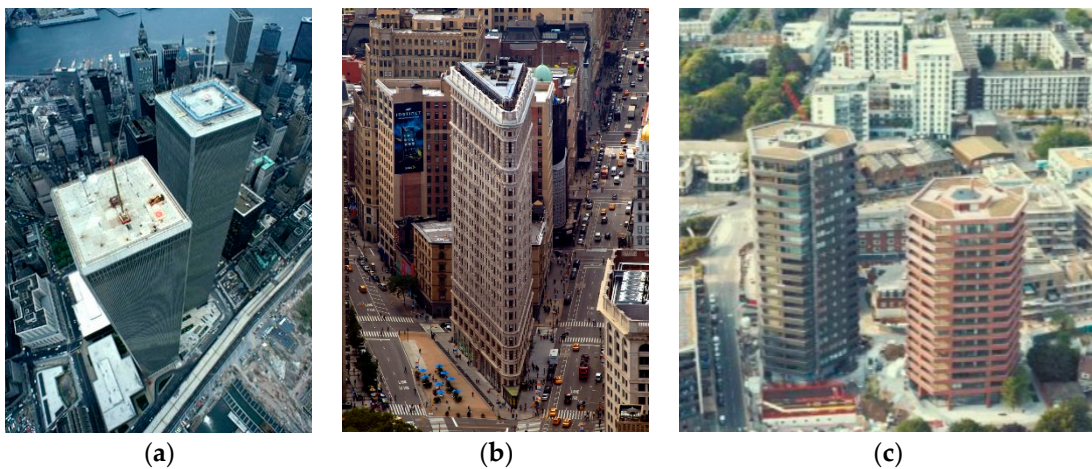


**Figure 2.** Three example pictures of: (a) rectangular plan building (WTC buildings, New York, USA) [23], (b) triangular plan building (Flatiron Building, New York, USA) [24] and (c) hexagonal plan building (Hoxton Press towers, London, UK) [25].

**Table 1.** Terminology of models.

Number of Stories	Rectangular Plan	Triangular Plan	Hexagonal Plan
20	20R	20T	20H
40	40R	40T	40H
60	60R	60T	60H
80	80R	80T	80H

The spaces between columns are normal (10 m in rectangular and triangular plans and 5 m in hexagonal plans) on the first floor, due to the existence of entrances, and the circumference of the second floor is also isolated by deep beams. As a result, the tubular behavior of framed tube structures begins from the third floor. To obtain an accurate analogy, the equivalent length of 30 m for each side of the rectangular and triangular plans is assumed which is equal to the hexagonal plan diameters. Specifically, each side of the hexagonal plan is obtained as 15 m. The distances between columns in the first floor are 10 m for rectangular and triangular plans and five meters for hexagonal plans. The spaces between peripheral columns, which create a tubular form in the structures, are 2.5 m in all stories. The dimensions of all circumferential and gravitational beams and columns are lessened in each 10 stories from the bottom to top of the structures.

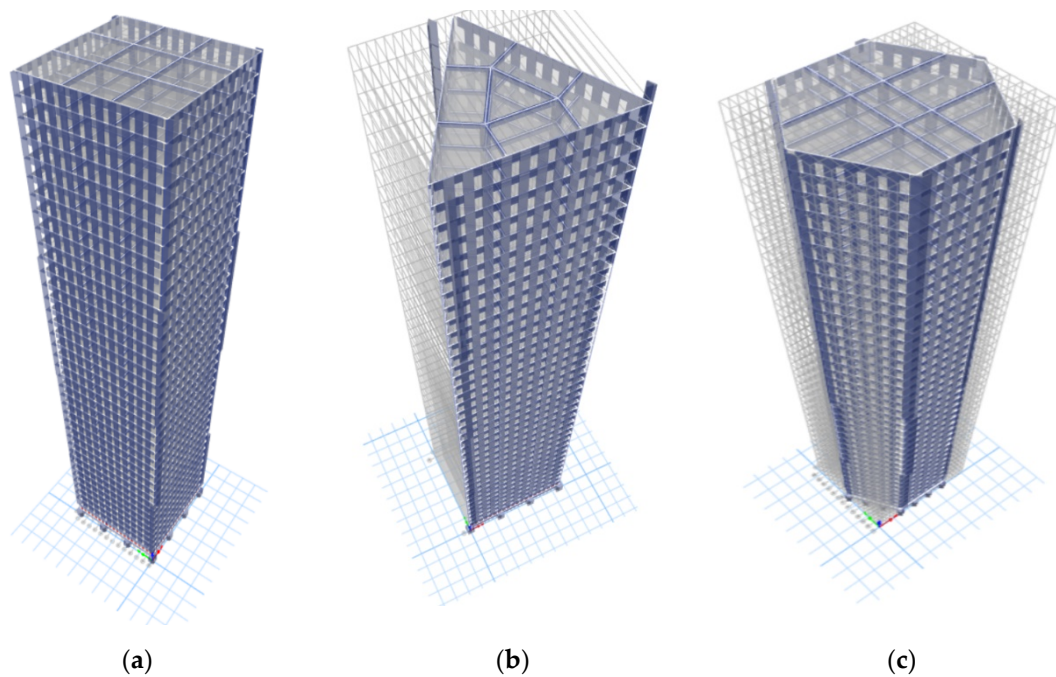


**Figure 3.** Three-dimensional view of 40-story models in ETABS Software: (a) rectangular, (b) triangular and (c) hexagonal.

### 3.2. Loading, Structural Analyses and Final Design Specifications

The national Iranian building code was used in order to calculate the loading of structures [26]. The total dead load for each model was  $308 \text{ kg/m}^2$  with regard to this point that ETABS software automatically calculates result loads from beams, columns and slabs weights. The dead load consisted of two parts— $63 \text{ kg/m}^2$  for floor weight and  $245 \text{ kg/m}^2$  for partition weight. Moreover,  $250 \text{ kg/m}^2$  was assumed as a live load.

The structures were analyzed by both static and pseudo-spectral dynamic methods, and to achieve a real and accurate structural analysis and design, earthquake and wind load were also applied separately on every 12 framed tube structures. The earthquake load was applied based on the Iranian seismic code [27], and the wind load specifications were according to the ASCE 7-16 code [28].

#### 3.2.1. Earthquake Load

In this study, all the models were analyzed against the earthquake load in two manners—static equivalent and pseudo-spectral dynamic analyses—and the Iranian seismic code was used for both methods.

##### Static Equivalent Earthquake Load

Like every static equivalent analysis, the equivalent static base shear in this research was determined in accordance with the following equations [27]:

$$V = CW \quad (1)$$

where  $V$  is base shear,  $C$  is the seismic response coefficient and  $W$  is the effective weight of building (all dead load + a percentage of live load)

And:

$$C = \frac{ABI}{R} \quad (2)$$

where  $A$  is the design basis acceleration over the bedrock dependent on the seismic zone of the building's location;  $B$  is the reflection coefficient of the building related to seismic zone, soil type and vibration period of the structure ( $T$ ) (See Figure 4);  $I$  is the importance factor; and  $R$  is the response modification factor which determines the nonlinear performance of the building during earthquakes and affected directly from the type of the structural system. It should be noticed that the structural system of the modeled structures is reinforced concrete special moment frames.  $A$ ,  $I$  and  $R$  were considered as 0.3, 1.0 and 10, respectively, due to the Iranian seismic code. The minimum value of  $V$  was  $V_{min} = 0.12AIW$  [27].

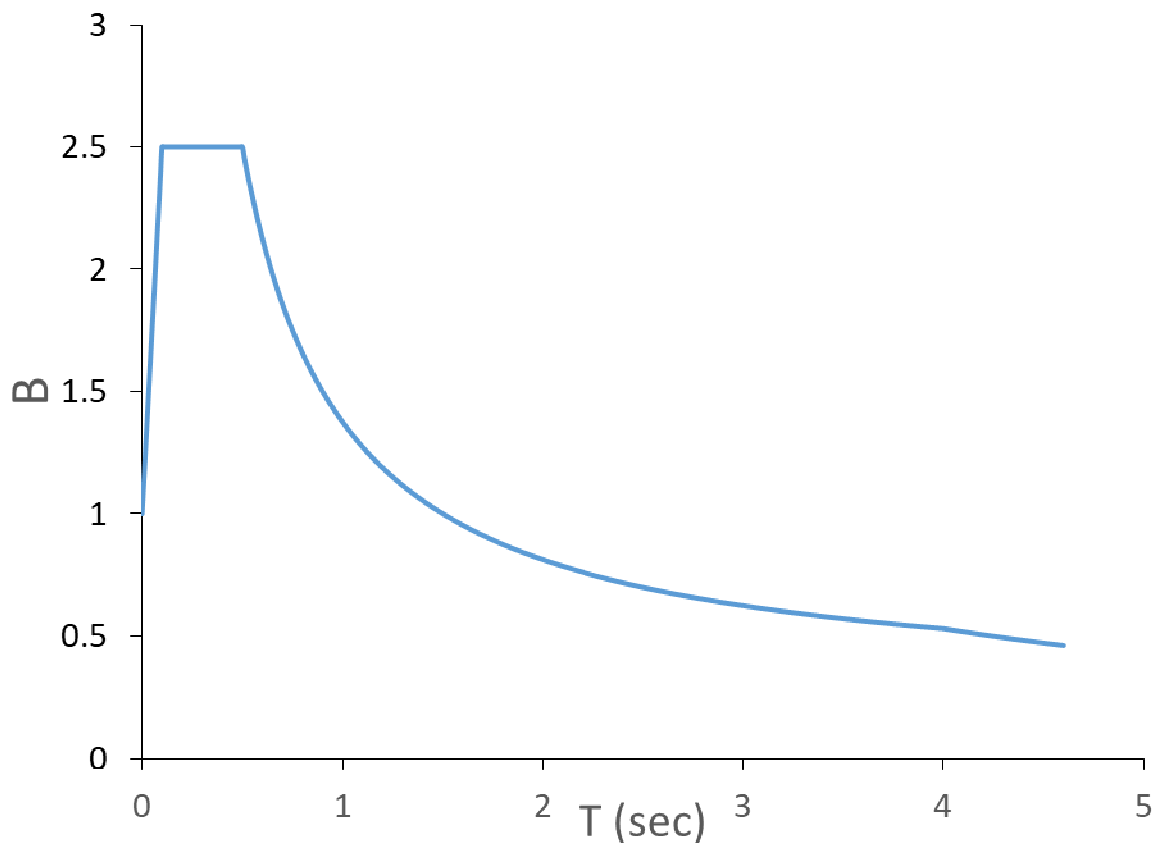


**Figure 4.** Response spectra intended for dynamic analysis (Iranian seismic code, 2015).

#### Dynamic Earthquake Load

In the dynamic analysis procedure, the lateral seismic load is determined from the dynamic response of a building subjected to an appropriate ground motion, and the pseudo-spectral dynamic analysis method was used in this paper according to the Iranian seismic code. The dynamic analysis spectrum was also obtained from the same code reflecting the effects of ground motion for design earthquake level. The spectrum shape is based on the type of soil, seismic zone and period of the structures. The information about the spectrum used in the dynamic analysis is shown in Figure 4 [27].

#### Wind Load

Wind load was applied to the aforementioned structures to obtain more accurate results and a comparison of framed tube behavior against different load types. Table 2 shows the specifications of the wind load obtained from the ASCE7-16 code [28].

**Table 2.** Specification of the wind load.

Parameters and Descriptions	Values
Basic wind speed, $V$	60 (m/s)
Exposure category	B
Importance factor	1
Directionality factor, $K_d$	0.85
Topographic factor, $K_{zt}$	1
Gust factor, $G_f$	0.85
Windward coefficient, $C_p$	0.8
Leeward coefficient, $C_p$	0.5

### 3.2.2. Specifications of the Models

To evaluate and analyze all 12 framed tube structures against earthquake and wind load, ETABS software version 9.7.3 was used. This choice was not made because the above software is developed specifically for analysis and design of building structures, but it also has a high ability for static and dynamic analyses regardless of the number of nodes and stories. The models were checked to have the minimum requirements of CSA 2019 code [29]. Circumferential columns and beams dimensions were lessened due to economic targets after every tenth story as the structures increased in height.

## 4. Results and Discussions

In this section, the results obtained from the static and dynamic analyses are discussed, and possible relationships between shear lag and the three different factors are studied in three sections. As was mentioned in the previous sections, the shear lag factor is the ratio of the axial force in a corner column to the middle column axial force in each story. It is worth mentioning that shear lag factors above one are referred to as positive shear lag and below one are referred to as negative. In the first part, the effect of lateral load types on the shear lag of framed tube structures is investigated. For this purpose, three types of lateral load including wind load, static earthquake load and dynamic earthquake load were considered to be subjected to the models. In the second section, the effects of plan geometry on the shear lag of tubular structures were studied and three different plan geometries with different heights were analyzed against different lateral loads. In the last section, the effects of height in framed tube structures on shear lag phenomena were discussed without considering any other factors.

### 4.1. The Effect of Lateral Load Type on Shear Lag of Framed Tube Structures

There was ample evidence from analysis results, which indicated that wind load could distribute forces among the columns more unequally. In most cases, shear lag phenomenon observed in structures subjected to the wind load were more severe than those for structures subjected to the dynamic or static earthquake load. Wind load in comparison with dynamic earthquake load caused a greater positive shear lag factor in almost all models. The positive Shear Lag factor obtained from the wind load for the 20R model was almost 1.5 times greater than the same factor for the same model against the dynamic earthquake load. Negative shear lag intensity of the 20R model against wind load was 1.22 times more than the same model subjected to the dynamic earthquake load. Although positive shear lag factors calculated from structures subjected to the wind load and dynamic earthquake load for 20T and 20H models were almost equal, negative shear lag factors for these structures subjected to the wind load were 39.08% and 21.18% more than the same models subjected to the dynamic earthquake load. The intensity of positive and negative shear lag factors observed from the 40R model subjected to the wind load was higher than the factors calculated from this model against dynamic earthquake load by 19.59% and 33.85%, respectively. The above percentages for 40T model were 3.3% and 25.71% and, for the 40H model, were 0.0% and 5.59%, respectively. This trend was observed for 60- and 80-story structures as well, and shear lag factors in structures subjected to wind load had greater amounts. Table 3 shows the percentage differences between shear lag obtained from wind load and dynamic

earthquake load. The nature of wind load and its distribution and application on the surface of the structure in comparison with the seismic load applied on the center mas of the rigid diagram floors by ETABS could be the reason for the above differences illustrated in Table 3.

**Table 3.** The differences between shear lag obtained from the wind load and dynamic earthquake load.

Story	20R	20T	20H
Pos. Shear Lag differences	31.14%	0%	~0%
Neg. Shear Lag differences	18.39%	39.08%	21.18%
Story	40R	40T	40H
Pos. Shear Lag differences	19.59%	3.31%	~0%
Neg. Shear Lag differences	33.85%	25.71%	5.95%
Story	60R	60T	60H
Pos. Shear Lag differences	6.03%	6.84%	0.98%
Neg. Shear Lag differences	6.85%	10.26%	~0%
Story	80R	80T	80H
Pos. Shear Lag differences	5.22%	2.78%	0%
Neg. Shear Lag differences	4.295	6.41%	2.20%

Moreover, although the dynamic analysis shows a more accurate result in comparison with equal static analysis, the shear lag factors for structures subjected to the static earthquake load were also less than those factors for structures subjected to the wind load in more than 80% of the models.

4.2. The Effect of Geometry of Plan on Shear Lag of Framed Tube Structures

Analysis results indicated that the amount of shear lag in framed tube structures could be highly dependent on the plan geometry of the structure. Shear lag diagrams for three types of 80-story framed tube structures subjected to earthquake loads are shown in Figures 5 and 6. Although these diagrams are more similar to a straight line in a particular story, the framed tube structure has less shear lag in that story. Diagrams with a minimum in the middle represent the positive shear lag, and those with a maximum in the middle illustrate negative shear lag.

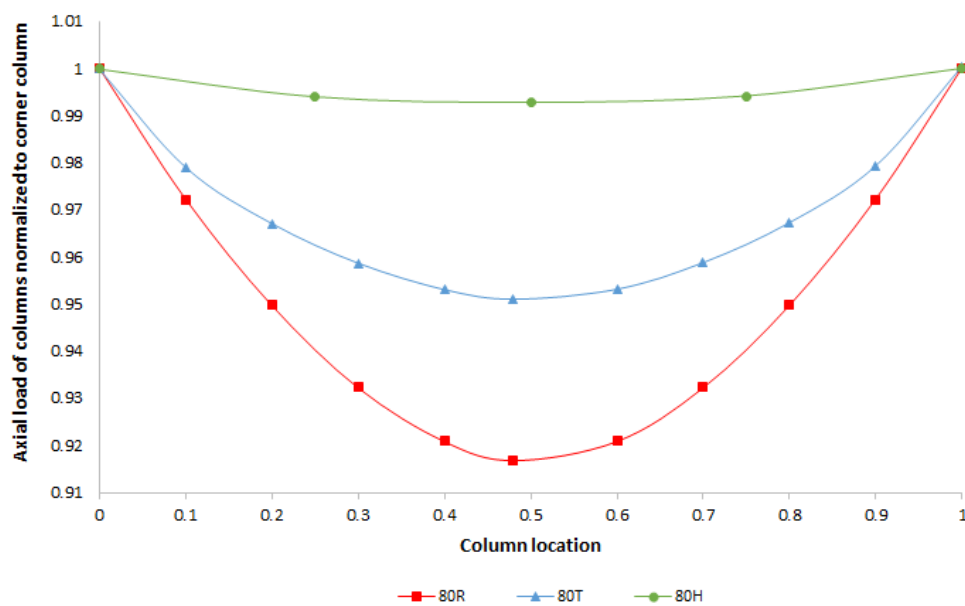


**Figure 5.** Shear lag diagram of 20th story of 80 story models subjected to the dynamic earthquake load.



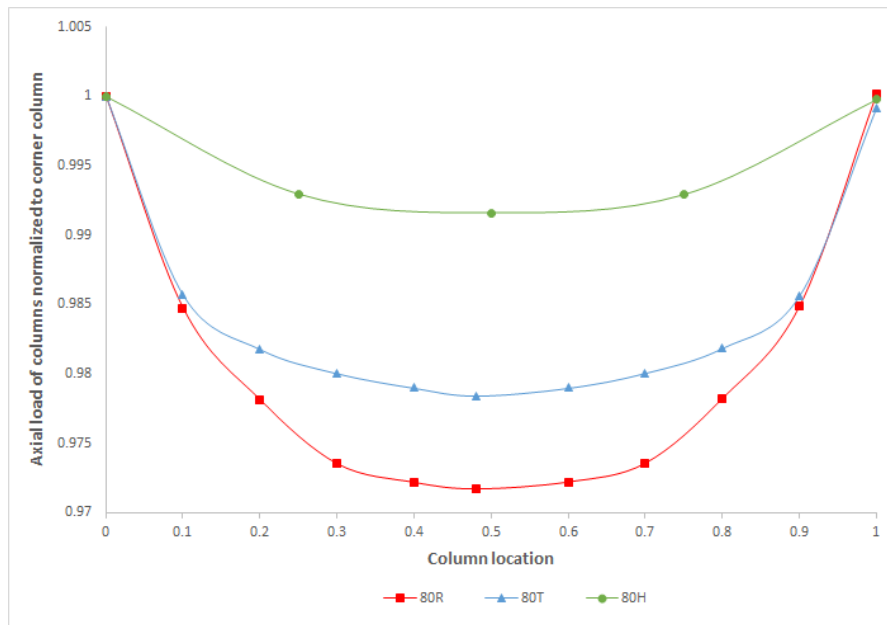


Figure 6. Shear lag diagram of 60th story of 80 story models subjected to the dynamic earthquake load.

According to these diagrams, it is observed that hexagon shaped plan structures have a better performance in terms of shear lag in comparison with the other two shapes. This structural behavior is in line with a previous study conducted by Awida, who stated that the octagon shape as a plan geometry can be the best in the structural response against wind load in comparison with other possible plan geometries [30]. Triangular-shaped structures act much better against lateral loads than rectangular ones which have the most inequality of load distribution in their flange columns. In addition, shear lag factors for every 10 stories in all structures were obtained, and the average of positive and negative shear lag factors for each structure was calculated as shown in Table 4. This table shows a similar trend in the case of shear lag in all structures. For instance, in terms of positive shear lag of a dynamic earthquake load, the 80H model acted 8.2% better than the 80R model. Moreover, the 80T model had 3.6% less shear lag in comparison with 80R. Furthermore, the negative shear lag factor of the 80H and 80T models—23% and 10.2%, respectively—performed better than the 80R model.

Table 4. The average of positive and negative shear lag factor in all models analyzed with three different load types.

Story	Dynamic Earthquake		Static Earthquake		Wind	
	Pos	Neg	Pos	Neg	Pos	Neg
20R	1.99	0.87	1.99	1.99	2.89	0.71
20T	1.74	0.87	1.73	1.73	1.74	0.53
20H	1.13	0.85	1.13	1.13	1.14	0.67
40R	1.19	0.65	1.24	1.24	1.48	0.43
40T	1.17	0.7	1.21	1.21	1.21	0.52
40H	1.02	0.84	1.01	1.01	1.01	0.79
60R	1.09	0.73	1.1	1.1	1.16	0.68
60T	1.09	0.78	1.1	1.1	1.17	0.7
60H	1.01	0.85	1.01	1.01	1.02	0.86
80R	1.09	0.7	1.15	1.15	1.15	0.67
80T	1.05	0.78	1.09	1.09	1.08	0.73
80H	1	0.91	1	1	1	0.89

To obtain a better understanding of shear lag fluctuation in the models, shear lag factors for odd stories were investigated, and Figures 7–9 shows the shear lag factor diagram for 80-story structures for three types of loads. In regard to these Figures, the shear lag factor diagrams for hexagonal-shaped plan structures in most of the stories are close to one, which means shear lag is at a minimum in these types. The shear lag phenomenon that showed up in rectangular-shaped plan structures was the maximum, especially in the first and last 10 stories. Furthermore, triangular-shaped plan structures exhibited a better behavior, in general, in terms of shear lag in comparison with rectangular ones mostly in the top half of the buildings, but still, shear lag in these structures was far higher than framed tube structures with hexagonal plan shape.

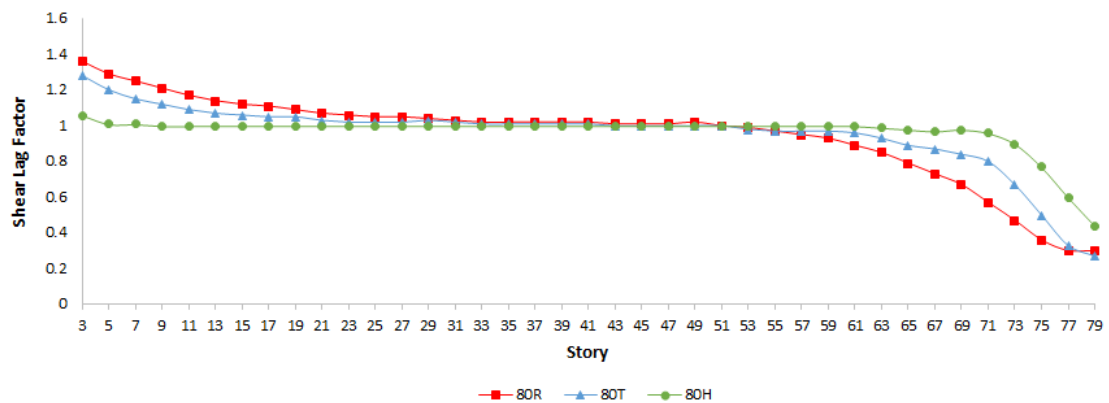


Figure 7. Shear lag factor diagram for 80 story structures subjected to the dynamic earthquake load.

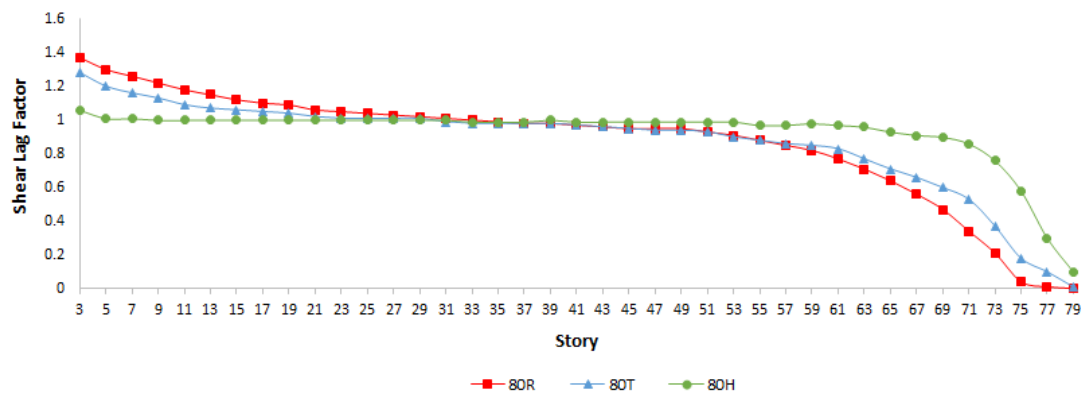


Figure 8. Shear lag factor diagram for 80 story structures subjected to the static earthquake load.

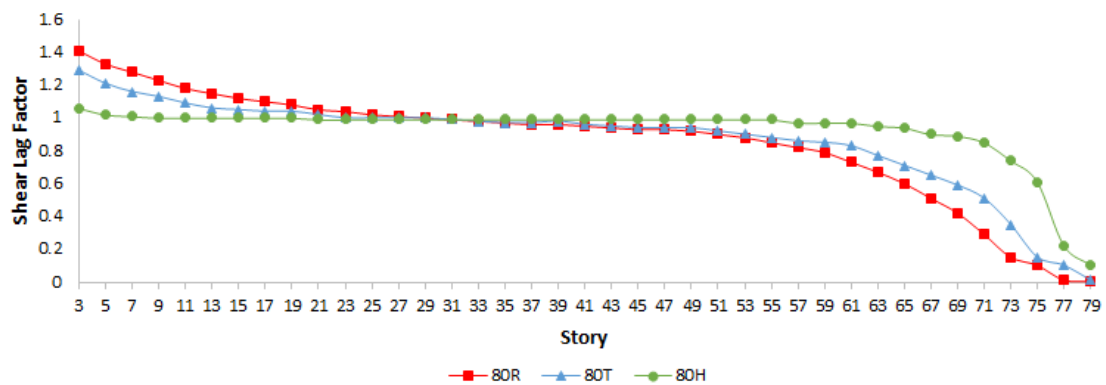


Figure 9. Shear lag factor diagram for 80 story structures subjected to the wind load.

Shear lag factors for static earthquake load are also available in Table 4. A lower positive shear lag up to 13% in the 80H model in comparison with 80R could be observed, and the 80T model had 5.21% less positive shear lag in comparison with 80R. This amount of reduction in negative shear lag was 21.3% for 80H model and 5.4% for 80T model as compared to the 80R model. This tendency could be observed in all the other models.

In addition to the earthquake load, lateral wind load was also applied to the structures in the static analysis method. The behavior in shear lag reduction in this part of analysis is also like previous sections (See Table 4). For positive shear lag, 80H and 80T specimens—13% and 6%, respectively—behaved better than the 80R model. Likewise, for negative shear lag, the 80H model responded at 24.7%, and the 80T model responded almost 8.2% better than 80R structures.

It is evident that from Figure 7, the shear lag effect is more intense in the top half of the structures, and this trend was observed in all other models. The shear lag switch-level from positive to negative in 20-story structures is between the 10th to 15th floors, for 40-story structures is between the 25th to 30th floors, for 60-story structures is between the 35th to 40th floors, and for 80-story structures is between the 45th to 50th floors.

#### 4.3. The Effect of Structural Height on Shear Lag of Framed Tube Structures

Structural height in tubular buildings has a direct effect on shear lag phenomenon. As the height of a framed tube structure increases, the positive shear lag in each story will decrease as well.

Table 5 indicates that 20 story structures had the highest positive shear lag factor in all types of plan geometry. This factor decreased as the number of stories increased almost in all the subsequent models. For example, the positive shear lag factor for 20R model against the dynamic earthquake load was 1.99, and this number was 1.19, 1.09 and 1.09 for 40R, 60R and 80R models, respectively. Furthermore, the average of positive shear lag factors for all models subjected to various lateral loads, without considering their plan geometry, is shown in Table 5. It is observed that positive shear lag factors in taller structures are fewer than this factor in shorter models and has nothing to do with the factor of geometry. In addition, the average of positive shear lag factors without considering any other factor such as load type and plan geometry was calculated. The positive shear lag factor in 20-story structures was 31.91% fewer than in 40-story structures, 37.02% fewer than in 60-story structures and 37.92% fewer than in 80-story structures. It is concluded that the positive shear lag phenomenon has a negative correlation with the height in framed tube structures subjected to any type of lateral load and with any plan geometry.

**Table 5.** Average of positive shear lag factor among three types of plan geometry for each height.

Story/Load Type	20 Story	40 Story	60 Story	80 Story
Dynamic Earthquake	1.62	1.13	1.06	1.05
Static Earthquake	1.62	1.15	1.07	1.08
Wind	1.92	1.23	1.12	1.08

#### 4.4. Comparison and Verification of the Results

In this study, a 40-story reinforced concrete framed tube building was chosen to compare the Matrix method [31] and Haji-Kazemi and Company [13] analyses results. Beams and columns dimensions in this example are  $0.8 \times 0.8$  m. Each story is 3 m in height, and center to center spacing between columns is 2.5 m. The modulus of elasticity and shear modulus of concrete are 20 and 8.0 GPa, respectively. The external load is 120 kN/m and uniformly distributed along the height of the structure. Figures 10 and 11 show the axial forces in columns of the web and flange of the structure at the base and 10th floor of the framed tube, respectively.

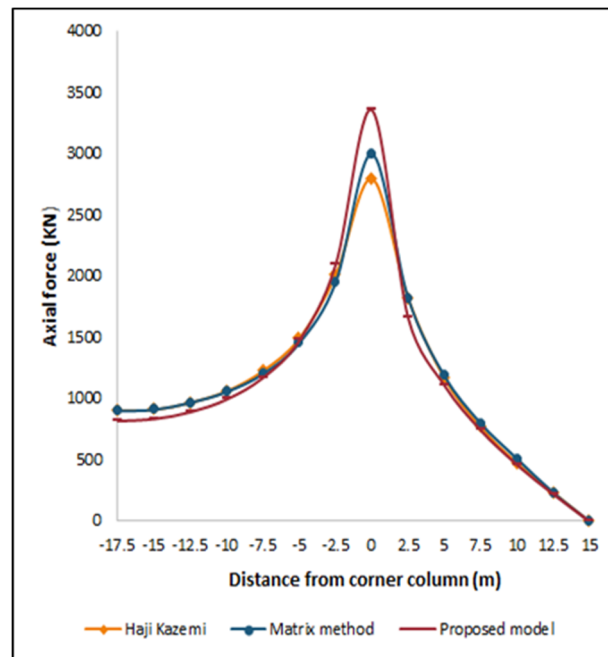


**Figure 10.** Axial force distribution in the flange and web columns at the base of the building.

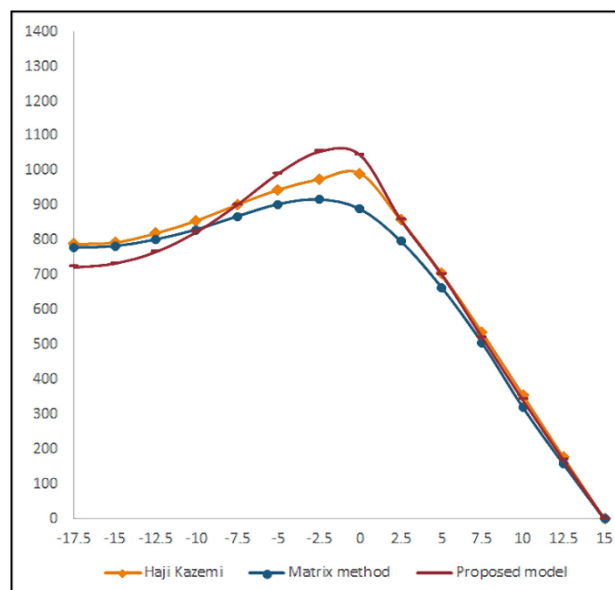


**Figure 11.** Axial force distribution in the flange and web columns at the 10th floor of the building.

Due to the symmetry of the structure, only half of the web and flange was considered. These diagrams illustrate that the axial forces in corner columns obtained from the proposed model have 9% and 10% difference in comparison with Haji-Kazemi and Company [13] and the Matrix method [31], respectively. In all models and analyses, the shear lag phenomenon was positive at lower heights and negative in the upper stories. Specifically, this anomaly was at a minimum in the middle of each structure.

This factor will decrease gradually in upper stories so that shear lag factor in the middle of the structures decreases to 1 which is considered no shear lag. This trend had no change, and the shear lag factor reduced till the last story. In sharp contrast with lower floors, minimum and negative shear lag factors were obvious in the upper stories. The above results are consistent with the previous studies [6].

## 5. Conclusions

This study investigated the effect of lateral load type, plan geometry and height on shear lag behavior of framed tube structures. For this goal, 12 models in four different heights and three different plan geometry against three different load types were considered. From the structural analyses performed, it could be concluded that:

(1) Type of the lateral load could affect the distribution of forces in peripheral columns in tubular structures. Wind load caused a greater amount of positive shear lag in comparison with the dynamic earthquake load and the static earthquake load by 9% and 7.5%, respectively. These numbers for negative shear lag were 14% and 1.5%, respectively. In regard to the importance of wind load in the design of high-rise structures and the severity of shear lag in framed tube structures designed based on it, the above results should be seriously considered by structural designers.

(2) Shear lag phenomenon could be affected significantly by the geometry plan in framed tube structures. Hexagon shaped plan structures had a reasonable behavior against lateral loads. Specifically, the average of positive and negative shear lag factors in the three types of analyses were 28.76%, and 25% less in hexagon shaped plan structures, respectively, in comparison with the control model (rectangular-shaped plan). This superiority may lead the structures towards being more laterally load resistant, of lighter weight and more economical due to its equal load distribution in the whole frame.

(3) Rectangular-shaped plan structures had the most inequality of axial force distribution in the flange frame columns. In the above mentioned structures, the average of positive shear lag rose to near two and even more and the average of negative shear lag fell down to below 0.5 in some cases. These amounts of shear lag are not evident in any other shaped plans.

(4) The structures with triangular-shaped plan had almost the same amount of shear lag with rectangular-shaped plan structures in shorter buildings, but the triangular plan had a better behavior in terms of shear lag than the rectangular plan in taller structures. The triangular performed almost 5% better, in the case of positive, and 8.4% in the case of negative shear lag on average in comparison with the rectangular-shaped plan.

(5) Shear lag of framed tube structures is highly affected by the height of the structure. Column axial forces were distributed more unequally in shorter structures, and taller buildings had smaller amount of shear lag factors. It can be concluded that in taller buildings, the structural behavior of the box-shaped cantilever beam that represents the whole building is more similar to Euler–Bernoulli beam than the shorter building and, as it is known from theory of structures, the effect of shear lag in Euler–Bernoulli cantilever beams (taller buildings) is lower than the shorter ones.

**Author Contributions:** Formal analysis, S.T.; Funding acquisition, S.S.R.K. and M.P.; Investigation, S.T.; Project administration, M.M., S.T., S.S.R.K. and M.P.; Resources, M.M. and S.S.R.K.; Software, S.T.; Supervision, M.M.; Writing—review & editing, M.M. and S.T.; and All authors have read and agreed to the published version of the manuscript.

**Funding:** This work was funded by the Ministry of Education, Youth, and Sports of the Czech Republic and the European Union (European Structural and Investment Funds Operational Program Research, Development, and Education) in the framework of the project “Modular platform for autonomous chassis of specialized electric vehicles for freight and equipment transportation”, Reg. No. CZ.02.1.01/0.0/0.0/16\_025/0007293, as well as financial support from internal grants in the Institute for Nanomaterials, Advanced Technologies and Innovations (CXI), Technical University of Liberec (TUL).

**Acknowledgments:** The authors would like to acknowledge the financial support by Ministry of Education, Youth and Sports of the Czech Republic and the European Union (European Structural and Investment Funds—Operational Program Research, Development and Education), Reg. No. CZ.02.1.01/0.0/0.0/16\_025/0007293, as well as the financial support from internal grants in the Institute for Nanomaterials, Advanced Technologies and Innovations (CXI), Technical University of Liberec (TUL).

**Conflicts of Interest:** The authors declare no conflict of interest.

## References

1. Taranath, B.S. *Tall Building Design: Steel, Concrete, and Composite Systems*; CRC Press: New York, NY, USA, 2016.
2. Taranath, B.S. *Wind and Earthquake Resistant Buildings: Structural Analysis and Design*; CRC Press: New York, NY, USA, 2004; pp. 298–300.
3. Smith, B.S.; Coull, A. *Tall Building Structures Analysis and Design*; Wiley-Interscience: New York, NY, USA, 1991.
4. Lee, K.-K.; Guan, H.; Loo, Y.C. Simplified analysis of shear-lag in framed-tube structures with multiple internal tubes. *Comput. Mech.* **2000**, *26*, 447–458.
5. Ali, M.M.; Moon, K.S. Structural developments in tall buildings: Current trends and future prospects. *Archit. Sci. Rev.* **2007**, *50*, 205–223. [[CrossRef](#)]
6. Chang, S.T.; Zheng, F.Z. Negative shear lag in cantilever box girder with constant depth. *J. Struct. Eng.* **1987**, *113*, 20–35. [[CrossRef](#)]
7. Shiraishi, N.; Matsumoto, M.; Shirato, H.; Ishizaki, H. On aerodynamic stability effects for bluff rectangular cylinders by their corner-cut. *J. Wind Eng. Ind. Aerodyn.* **1988**, *28*, 371–380. [[CrossRef](#)]
8. Hayashida, H.; Iwasa, Y. Aerodynamic shape effects of tall building for vortex induced vibration. *J. Wind Eng. Ind. Aerodyn.* **1990**, *33*, 237–242. [[CrossRef](#)]
9. Connor, J.J.; Pouangare, C.C. Simple model for design of framed-tube structures. *J. Struct. Eng.* **1991**, *117*, 3623–3644. [[CrossRef](#)]
10. Kwan, A.K.H. Simple method for approximate analysis of framed tube structures. *J. Struct. Eng.* **1994**, *120*, 1221–1239. [[CrossRef](#)]
11. Han, S.W.; Oh, Y.H.; Lee, L.H. Structural performance of shear wall with sectional shape in wall-type apartment building. *J. Korea Concr. Inst.* **2000**, *12*, 3–14.
12. Lee, K.K.; Lee, L.H.; Lee, E.J. Prediction of shear-lag effects in framed-tube structures with internal tube (s). *Struct. Des. Tall Spec. Build.* **2002**, *11*, 73–92. [[CrossRef](#)]
13. Haji-Kazemi, H.; Company, M. Exact method of analysis of shear lag in framed tube structures. *Struct. Des. Tall Spec. Build.* **2002**, *11*, 375–388. [[CrossRef](#)]
14. Moghadasi, M.; Keramati, A. Effects of adding internal tube(s) on behavior of framed tube tall buildings subjected to lateral load. In Proceedings of the 7th Asia Pacific Structural Engineering and Construction Conference (APSEC) and 2nd European Asian Civil Engineering Forum (EACEF), Langkawi, Malaysia, 25 July 2009; Volume 1.
15. Shin, M.; Kang, T.H.K.; Pimentel, B. Towards optimal design of high-rise building tube systems. *Struct. Des. Tall Spec. Build.* **2012**, *21*, 447–464. [[CrossRef](#)]
16. Mazinani, I.; Jumaat, M.Z.; Ismail, Z.; Chao, O.Z. Comparison of shear lag in structural steel building with framed tube and braced tube. *Struct. Eng. Mech.* **2014**, *49*, 297–309. [[CrossRef](#)]
17. Nagvekar, Y.D.; Hampali, M.P. Analysis of shear lag effect in hollow structures. *Int. J. Eng. Res. Technol.* **2014**, *3*, 936–937.
18. Szolomicki, J.; Golasz-Szolomicka, H. Technological Advances and Trends in Modern High-Rise Buildings. *Buildings* **2019**, *9*, 193. [[CrossRef](#)]
19. Alaghmandan, M.; Elnimeiri, M.; Krawczyk, R.J.; Buelow, P.V. Modifying Tall Building Form to Reduce the Along-Wind Effect. *CTBUH J.* **2016**, *1*, 34–39.
20. Shi, Q.; Zhang, F. Simplified calculation of shear lag effect for high-rise diagrid tube structure. *J. Build Eng.* **2019**, *22*, 486–495. [[CrossRef](#)]
21. Hentz, S.; Donzé, F.V.; Daudeville, L. Discrete Element modeling of concrete submitted to dynamics loading at high strain rates. *Comput. Struct.* **2004**, *82*, 2509–2524. [[CrossRef](#)]
22. Golewski, G.; Sadowski, T. Fracture toughness at shear (Mode II) of concretes made of natural and broken aggregates. *Brittle Matrix Compos.* **2006**, *8*, 537–546. [[CrossRef](#)]
23. Dec. 23, 1970: World Trade Center Tops Out. Available online: <https://www.wired.com/2008/12/dayintech-1223/> (accessed on 2 October 2020).
24. Hoxton Press. N1. Available online: <https://www.homeviews.com/development/hoxton-press-n1/> (accessed on 2 October 2020).
25. The Skyscraper Center. Available online: <http://www.skyscrapercenter.com/building/flatiron-building/9014> (accessed on 2 October 2020).

26. *National Iranian Buildings Code, Part 6, Loads on Structures*; BHRC Publication: Tehran, Iran, 2009.
27. *Iranian Code of Practice for Seismic Resistant Design of Buildings*, 4th ed.; BHRC Publication: Tehran, Iran, 2015.
28. *Minimum Design for Buildings and Other Structures*; American Society of Civil Engineering (ASCE7-16 Standard): Fairfax, VA, USA, 2016.
29. *Design of Concrete Structures for Buildings*; Canadian Concrete Code (CSA A.23.3-19): Toronto, ON, Canada, 2019.
30. Awida, T.A. Impact of Building Plan Geometry on the Wind Response of Concrete Tall Buildings. In Proceedings of the Modern Methods and Advances in Structural Engineering and Construction (ISEC-6), Zurich, Switzerland, 21–26 June 2011.
31. Ha, K.H.; Moselhi, O.; Fazio, P. Orthotropic membrane for tall building analysis. *J. Struct. Div. ASCE* **1978**, *104*, 1495–1505.



© 2020 by the authors. Licensee MDPI, Basel, Switzerland. This article is an open access article distributed under the terms and conditions of the Creative Commons Attribution (CC BY) license (<http://creativecommons.org/licenses/by/4.0/>).